J Nanopart Res (2018) 20:127
https://doi.org/10.1007/s11051-018-4233-3

RESEARCH PAPER

Magnetic Pd nanocatalyst Fe_3O_4@Pd for C–C bond formation and hydrogenation reactions

Catalina Biglione · Ariel L. Cappelletti · Miriam C. Strumia · Sandra E. Martín · Paula M. Uberman

Received: 8 January 2018 / Accepted: 20 April 2018

Abstract Small core-shell Fe_3O_4@Pd superparamagnetic nanoparticles (MNPs) were obtained with good control in size and shape distribution by metal-complex thermal decomposition in organic media. The role of the stabilizer in the synthesis of MNPs was studied, employing oleylamine (OA), triphenylphosphine (TPP) and triphenylamine (TPA). The results revealed that, among the stabilizer investigated, the presence of oleylamine in the reaction media is crucial in order to obtain an uniform shell of Pd(0) in Fe_3O_4@Pd MNPs of 7 ± 1 nm. The synthesized core-shell MNPs were tested in Pd-catalyzed Heck-Mizoroki and Suzuki-Miyaura coupling reactions and *p*-chloronitrobenzene hydrogenation. High conversion, good reaction yields, and good TOF values were achieved in the three reaction systems with this nanocatalyst. The core-shell nanoparticle was easily recovered by a simple magnetic separation using a neodymium commercial magnet, which allowed performing up to four cycles of reuse.

Keywords Nanocatalysis · Pd nanoparticle · Core-shell synthesis · Fe_3O_4

Electronic supplementary material The online version of this article (https://doi.org/10.1007/s11051-018-4233-3) contains supplementary material, which is available to authorized users.

C. Biglione · A. L. Cappelletti · M. C. Strumia · S. E. Martín · P. M. Uberman
Universidad Nacional de Córdoba, Facultad de Ciencias Químicas, Departamento de Química Orgánica, Haya de la Torre esq. Medina Allende, X5000HUA Córdoba, Argentina

C. Biglione · A. L. Cappelletti · M. C. Strumia
Instituto de Investigación y Desarrollo de Ingeniería de Procesos y Química Aplicada (IPQA)-CONICET, Departamento de Química Orgánica, Facultad de Ciencias Químicas, Universidad Nacional de Córdoba, X5000HUA Córdoba, Argentina

S. E. Martín · P. M. Uberman (✉)
Instituto de Investigaciones en Fisicoquímica de Córdoba (INFIQC)-CONICET, Departamento de Química Orgánica, Facultad de Ciencias Químicas, Universidad Nacional de Córdoba, X5000HUA Córdoba, Argentina
e-mail: uberman@fcq.unc.edu.ar

Introduction

The formation of C–C bond is one of the major goals in modern organic synthesis. In this context, Pd-catalyzed coupling reactions, like Heck-Mizoroki reactions, had excelled as efficient methods for the construction of C–C bonds (Torborg and Beller 2009; Yin and Liebscher 2007; Dounay and Overman 2003). These reactions usually are performed using soluble Pd complexes, in which phosphines and other ligands are used to produce stable catalytic species in the reaction medium (Martin and Buchwald 2008; Fu 2008; Kantchev et al. 2007; Meijere and Diederich 2004; Beletskaya and Cheprakov 2009). However, homogeneous catalysts suffer from several practical disadvantages, such as difficult catalyst separation and recycling, as well as the presence of toxic metal in the final organic product (Garrett and Prasad 2004).

In this regard, significant improvements have been achieved with the introduction of nanocatalysis. This emerging field represents a merger between classical catalysis methodologies, since it combines the surface activity of heterogeneous catalysts (due to their large

Published online: 04 May 2018

surface area-to-volume ratio characteristic of nanomaterials) with exceptional fine tuning of homogeneous catalysts (by modifying nanoparticle variables like size, composition, morphology, and protective capping agents) (Polshettiwar 2013; Astruc et al. 2005). Several supported and colloidal Pd nanoparticles (Pd NPs) were successfully used in many Pd-coupling reactions (Deraedt and Astruc 2014; Fihri et al. 2011; Jin and Lee 2010; Astruc 2007), achieving softer reaction conditions, higher selectivity, and larger TOF values. However, non-supported nanocatalysts have the disadvantage of limited reuse and recyclability (Yin and Liebscher 2007; Polshettiwar and Varma 2010; Leadbeater and Marco 2002).

In this sense, catalyst recyclability was improved by the use of using superparamagnetic nanoparticles (MNPs) as support for Pd catalysts (Nasir Baig et al. 2015; Zhang et al. 2012a, Polshettiwar et al. 2011). The insoluble nature and superparamagnetic behavior of MNPs enable easy and efficient separation from reaction mixture, by only application of an external magnetic field. Among the common MNPs used as catalyst supports, iron oxide materials such as magnetite (Fe_3O_4) have been widely employed (Rossi et al. 2014; Zhu et al. 2010). Although Fe_3O_4 MNPs can be easily prepared (Lee et al. 2013; Frey et al. 2009; Polshettiwar et al. 2009), they present some drawbacks like sensitive to oxidation, acid erosion, and thermal degradation (Rossi et al. 2014). Also, this type of nanomaterials tends to aggregate to form the thermodynamically favored bulk metal, decreasing considerably their surface area. To prevent undesired aggregation or degradation, iron oxide MNPs were usually surrounded by different stabilizer, such as a layer of inorganic material or molecular stabilizers (Kainz and Reiser 2014). Protection of magnetic content by coating the surface with a layer of inorganic material like modified silica or titania is usually employed (Atashkar et al. 2013; Jacinto et al. 2008; Wang et al. 2014b; Sobhani and Pakdin-Parizi 2014; Li et al. 2012; Zhang et al. 2011; Shylesh et al. 2010; Rosario-Amorinâ et al. 2009; Ceylan et al. 2008); however, these methodologies could involve complex synthesis and several steps (Wang et al. 2014b; Sobhani and Pakdin-Parizi 2014; Li et al. 2012; Zhang et al. 2011; Shylesh et al. 2010; Rosario-Amorinâ et al. 2009; Ceylan et al. 2008).

Magnetic nanocatalysts were also stabilized by using organic ligands containing functional groups like carboxylate, phosphonate, phosphines, amine, or thiol (Rossi et al. 2014; Lee et al. 2013; Mori and Yamashita 2011). In addition to their protecting role, these stabilizers can tune the reactivity of nanocatalysts by influencing their morphology and surface chemistry, which could lead in many cases to a decrease in catalytic activity (Wang et al. 2014a; Mazumder and Sun 2009).

Another innovative approach consists in designing MNPs in which Fe_3O_4 was in the inner core and a metallic shell was incorporated onto the magnetic NPs (Lyon et al. 2004; Xu et al. 2007). This type of core-shell structure protects the inner core against external aggression and allowed to combine the properties of both metals. Furthermore, important advantages in catalysis were accomplished by using core-shell NPs. Due to the catalytic reaction that takes place on the surface of the nanocatalyst, only a small fraction of atoms is mainly active in a catalytic process. Thus, achieving NPs in which the inner atoms could be replaced by non-noble metals provides an alternative for optimizing the use of the noble metal (Ferrando et al. 2008; Zaleska-Medynska et al. 2016; Metin et al. 2013). Nevertheless, Pd NPs directly supported over the magnetic core have been less explored as catalysts. These types of Pd MNPs exhibited good catalytic activity and Pd directly supported on the surface of Fe_3O_4 showed negligible effect on the magnetic properties of the support (Kim and Song 2014; Senapati et al. 2012; Zhang et al. 2012a, b; Laska et al. 2009; Liu et al. 2008). Recently, we described a new synthesis for core-shell Fe_3O_4@Pd MNPs stabilized with oleylamine (OA). It was demonstrated that the Pd(0) shell protects the magnetic core against oxidation and degradation (Cappelletti et al. 2015). The catalytic activity of Fe_3O_4@Pd-OA MNPs was evaluated in the Suzuki-Miyaura cross-coupling reaction for *p*-iodoanisole and *p*-fluorophenylboronic acid, exhibiting good catalytic activity and recyclability.

Following our increasing interest in the development of novel metal nanocatalysts and evaluation of their practical application in organic chemistry, herein we explored core-shell Fe_3O_4@Pd-OA MNPs nanocatalyst in Heck-Mizoroki and Suzuki-Miyaura cross-coupling reactions for the synthesis of stilbenes and biaryl compounds. Furthermore, to extend the scope of this catalyst, the catalytic activity of these MNPs in the hydrogenation of *p*-chloronitrobenzene was studied. In addition, we examined the stabilizer effect on the synthesis and catalytic activity of core-shell Fe_3O_4@Pd. Since OA ligand can strongly bind to the surface, occupying some active sites in the nanocatalyst surface and limiting

their catalytic activity, Fe_3O_4@Pd MNPs were synthesized in the presence of other capping agents.

Experimental

Reagents and instrumentation

Urea (U, 99.99%), $Fe(NO_3)_3 \cdot 9H_2O$ (99.999%), $Pd(Acac)_2$ (99%), oleylamine (OA, 70%), triphenylamine (TPA), triphenylphosphine (TPP), dibenzyl ether (DBE, ≥ 98%), absolute ethanol (EtOH, ≥ 99.5%), n-hexane anhydrous (95%), diethyl ether (≥ 99.0), *p*-iodoanisole (98%), *p*-iodotoluene (98%), *o*-iodotoluene (98%), p-iodobenzotrifluoride (98%), iodobenzene (99%), *p*-iodoaniline (98%), *p*-bromobenzophenone (98%), *p*-bromoacetophenone (98%), *p*-bromobenzonitrile (99%), styrene (97%), 4-vinylpiridyne (99%), phenylboronic acid (≥ 97.0%), *o*-methylphenylboronic acid (98%), *p*-fluorophenylboronic acid (≥ 97.0%), K_3PO_4 (≥ 98%), and Na_2SO_4 (≥ 99.0) were obtained from Sigma-Aldrich and used as received. Dimethylformamide (DMF) was stored with molecular sieves and then distilled under reduced pressure with bubbling of nitrogen. All catalytic reactions were carried out under N_2 atmosphere, unless otherwise noted. Silica gel (0.063–0.200 mm) was used in column chromatography. Gas chromatographic analysis was performed on a gas chromatograph with a flame ionization detector and equipped with the following column: VF-5 ms, 30 m × 0.25 mm × 0.25 μm. ^{1}H NMR and ^{13}C NMR were conducted on a High-Resolution Spectrometer Bruker Advance 400, in $CDCl_3$ as solvent. Gas chromatographic/mass spectrometer analysis was carried out on a GC/MS QP 5050 spectrometer equipped with a VF-5 ms, 30 m × 0.25 mm × 0.25 μm column. The characterization by powder X-ray diffraction (PXRD) was performed using a PANalytical X'Pert Pro diffractometer (40 kV, 40 mA), in Bragg–Brentano reflection geometry with Cu Kα radiation (λ = 1.5418 Å). The data were obtained between 20° and 70° (2θ) in steps of 0.02 and a counting time of 24 s. The refinement of the crystal structure was performed by the Rietveld method using the FULLPROF program. A pseudo-Voigt shape function was always adequate to obtain good fits for experimental data. Infrared spectroscopy (FT-IR) was carried out on a Nicolet-5SXC, using KBr pellets. Transmission electron microscopy was conducted in a JEM-Jeol 1120 operating at 80 kV, at the IFFIVE Research Institute, INTA, Córdoba, Argentina. The samples were prepared by dropping a dispersion of NPs diluted in cyclohexane onto an ultrathin carbon-coated copper grid. Determination of Pd content was performed in an ICP-MS Agilent series 7700, at ICYTAC-CONICET-Universidad Nacional de Córdoba.

Synthesis of Fe_3O_4 MNP seeds

Magnetite MNPs were prepared following the methodology described in our previous work (Cappelletti et al. 2015). In a typical reaction, Fe-urea complex (2.5037 g, 4.16 mmol) was dispersed in 20 mL of OA and 20 mL of DBE at room temperature under N_2 atmosphere. The dispersion was dehydrated by heating it at 120 °C for 40 min under magnetic stirring and then transferred to a dry three-necked round-bottom flask equipped with a reflux system, magnetic stirring, and N_2 atmosphere. The dispersion was heated to 155 °C (10 °C/min) for 1 h; later, the temperature was raised to 300 °C (10 °C/min) and kept for 60 min. The system was cooled down to room temperature, and then, aliquots of the resultant dispersion were transferred to a conical tube and diluted three times with absolute dry ethanol and centrifuged at 6000 rpm for 15 min. Finally, MNPs were washed with absolute ethanol (7 times) until no contaminants (OA, DBE, or reaction residues) were detected by FT-IR in the supernatant. After this, the powder was dried under vacuum at 45 °C for 12 h. The MNPs obtained were characterized by PXRD, FT-IR, TEM, and magnetization measurements.

Synthesis of Fe_3O_4@Pd MNPs

The core-shell MNPs have been prepared following a similar methodology described above for the preparation of magnetite MNPs. These MNPs were used as seeds for the growth of the shell of Pd(0) shell. Firstly, Fe_3O_4-OA (0.3828 g) and $Pd(Acac)_2$ (1.5222 g) was dispersed in 30 mL of OA and 30 mL of DBE. Then, the dispersion was magnetically stirred and heated to 200 °C (10 °C/min) and kept at this temperature for 1 h to allow the complete decomposition of the $Pd(Acac)_2$. Finally, the dispersion was cooled down to room temperature, and the core-shell MNPs were transferred to a conical tube and diluted three times with absolute dry ethanol and centrifuged at 6000 rpm for 15 min. The black powder was washed with absolute

ethanol until no remaining reagents (OA, DBE) were detected by FT-IR spectroscopy in the supernatant. The MNPs obtained were characterized by PXRD, FT-IR, TEM, and magnetization measurements.

MNPs with TPP or TPA were obtained by analogous synthesis as the one used for MNPs stabilized with OA, adding only 80 mL of DBE and 4.2 mmol of TPP/TPA. The MNPs obtained were characterized by PXRD, FT-IR, TEM, and magnetization measurements.

General procedure for the Heck-Mizoroki coupling reaction

Aryl halide (0.5 mmol), alkene (0.75 mmol), and K_2CO_3 (1.5 mmol) were added into a 25-mL Schlenk tube with Teflon screw-cap septum equipped with a magnetic stirrer and a N_2 inlet. Finally, 1 mL of a dispersion containing 1.9 mg of Fe_3O_4@Pd-OA MNPs (1.5%) per mL of DMF was added. The reaction mixture was heated in an oil bath at 115 °C. After being cooled to room temperature, the mixture was quenched by the addition of 2 mL of water and then extracted three times with ethyl acetate (3 mL each) and dried with anhydrous Na_2SO_4. The reaction was analyzed by GC and GC-MS. The product was purified by silica-gel column chromatography and characterized by ^{1}H NMR, ^{13}C NMR, and GC-MS. All reactions were quantified by GC analysis, by internal standard methods. All spectroscopic data agreed with those previously reported.

General procedure for the Suzuki-Miyaura cross-coupling reaction

Aryl halide (0.5 mmol), arylboronic acid (0.75 mmol), and K_3PO_4 (1.5 mmol) were added into a 25-mL Schlenk tube with Teflon screw-cap septum equipped with a magnetic stirrer, and a N_2 inlet, . Finally, 1 mL of a dispersion containing 1.9 mg of Fe_3O_4@Pd-OA MNPs (1.5%) per mL of DMF was added. The reaction was heated in an oil bath at 115 °C. After being cooled to room temperature, the mixture was diluted with 2 mL of water and extracted three times with ethyl acetate (3 mL each) and dried with anhydrous Na_2SO_4. The reaction was analyzed by GC and GC-MS and was quantified by GC analysis, by internal standard methods. The biaryl product was purified by silica-gel column chromatography and characterized by ^{1}H NMR, ^{13}C NMR, and GC-MS. All spectroscopic data agreed with those previously reported.

General procedure for the hydrogenation of p-chloronitrobenzene

p-chloronitrobenzene (**13**, 19.7 mg, 0.25 mmol) was added into a 25-mL round-bottomed flask followed by the addition of 1 mL of a dispersion containing 1.9 mg of Fe_3O_4@Pd MNPs (1.5%) in ethanol and $NaBH_4$ (1 mmol) in 2 mL of ethanol. The reaction was carried out at room temperature. The mixture was diluted with 2 mL of water and then extracted three times with ethyl acetate (3 mL each) and dried with anhydrous Na_2SO_4. The reaction was analyzed by GC and GC-MS. The product was purified by silica-gel column chromatography and characterized by ^{1}H NMR, ^{13}C NMR, and GC-MS. All these spectroscopic data agreed with those previously reported. All reactions were quantified by GC analysis, by internal standard methods.

Catalyst recycling experiment in Pd-catalyzed C–C coupling reaction

Recyclability test in Heck-Mizoroki coupling reaction between *p*-iodoanisole (**1a**) and styrene (**2**) catalyzed by Fe_3O_4@Pd-OA MNPs was evaluated. Initially, the reaction was carried out following the procedure previously described. After the reaction mixture was heated at 115 °C for 5 h, the catalyst was separated with a magnet and the crude reaction was removed. The MNPs were washed two times with ethyl ether. Then, fresh amounts of reactants and DMF were added to the MNPs. The experiment was performed four times by consecutive addition of a new batch of *p*-iodoanisole (**1a**, 0.5 mmol), styrene (**2**, 0.75 mmol), K_2CO_3 (0.5 mmol), and 1 mL DMF. The reaction mixture was then heated for another 5 h. The reaction was monitored by GC analyses.

A similar procedure was followed to evaluate recyclability in Suzuki–Miyaura coupling reaction between *p*-iodoanisole (**1a**) and phenylboronic acid (**7a**).

Characterization data of organic compounds

Products were characterized by ^{1}H NMR, ^{13}C NMR, and GC-MS. All spectroscopic data were in concordance with those previously reported for the following

compounds: (*E*)-1-methoxy-4-styrylbenzene (**3**) (Alacid and Nájera 2009), (*E*)-4-Aminostilbene (**4**) (Sun et al. 2010), (*E*)-1-methyl-4-styrylbenzene (**5**) (Quinteros et al. 2015), (*E*)-1-methyl-2-styrylbenzene (**6**) (Quinteros et al. 2015), (*E*)-1-styryl-4-(trifluoromethyl)benzene (**7**) (Quinteros et al. 2015), (*E*)-phenyl(4-styrylphenyl)methanone (**8**) (Alacid and Nájera 2009), (*E*)-1-(4-styrylphenyl) ethanone (**10**) (Alacid and Nájera 2009), (*E*)-4-(4-methylstyryl)pyridine (**11**) (Quinteros et al. 2015), (*E*)-1-(4-(2-(pyridin-4-yl)vinyl)phenyl)ethanone (**12**) (García et al. 2017), *p*-methoxybiphenyl (**14**) (Sahoo et al. 2004), *o*-methoxybiphenyl (**15**) (Sahoo et al. 2004), 4-fluoro-4′-methoxybiphenyl (**16**) (Sahoo et al. 2004), 1-(biphenyl-4-yl)ethanone (**17**) (Sahoo et al. 2004), and *p*-chloroaniline (**19**) (Cantillo et al. 2013).

Results and discussion

Catalyst preparation and characterization

The synthesis of core-shell Fe_3O_4@Pd MNPs was carried out as previously reported (Cappelletti et al. 2015). It is worth mentioning that analysis of HRTEM, Dark field images, magnetic characterization, and TGA confirms that this synthetic approach allowed obtaining well-defined core-shell structure with a thickness of the Pd shell of 1.25–1.35 nm. The synthetic procedure involved the preparation of Fe_3O_4 seeds, over which a Pd shell was deposited (Scheme 1). Thus, Fe_3O_4 seeds were achieved by thermal decomposition of Fe-urea complex in dibenzylether (DBE) and oleylamine (OA). Then, Pd shell was generated over the MNPs by thermal decomposition of $Pd(Acac)_2$ in the presence of the different stabilizers: oleylamine (OA) and triphenylphosphine (TPP). After purification, core-shell Fe_3O_4@Pd MNPs were obtained as black powders. Finally, all MNPs were characterized by PXRD and FT-IR.

FT-IR spectra acquired for all Fe_3O_4@Pd MNPs exhibited the typical signal of Fe–O tension from magnetite at 582 cm^{-1} (Fig. 1) (Hong et al. 2006). Typical signals of OA ligand (2925, 2854, and 1415 cm^{-1}) were detected in all MNPs. In addition, the FT-IR spectra of Fe_3O_4@Pd MNPs synthesized using TPP shows the characteristic signals of TPP: C–H sp^2 stretching (3060 cm^{-1}) and P–C stretching (744 cm^{-1}). These results can be explained considering the synthetic pathway followed to prepare Fe_3O_4@Pd MNPs. Since OA was used to stabilize the original magnetite seeds, the appearance of OA signals in the IR spectra of the final material indicates that OA ligand remained attached to the MNPs throughout the synthesis. This demonstrates the strong interaction of OA with the MNPs surface, and therefore, a ligand-like TPP was not able to remove it entirely from the MNP surface.

The analysis of the MNP composition was performed by PXRD (Fig. 2). For Fe_3O_4@Pd-OA MNPs, PXRD patterns exhibit the typical diffraction line of Fe_3O_4 phase at around 30.5°, 35.8°, 43.5°, 53.9°, 57.3°, and 62.9° (2θ), corresponding to reflections (220), (311), (400), (422), (511), and (440), respectively. In addition, signals were also identified at 39.8°, 46.1°, and 67.3° (2θ), corresponding to reflections (111), (200), and (220) of the fcc Pd phase. In the case of MNPs synthesized in presence of TPP, besides the PXRD pattern for Fe_3O_4 and Pd, an additional phase was detected at 33.9°, 45.9°, 56.8° (2θ) which can be indexed as (101), (110), and (112) phases of PdO (Fig. 2) (Bi and Lu 2003). In order to determine if the formation of the new phase was due to the presence of phosphorus atom in the ligand

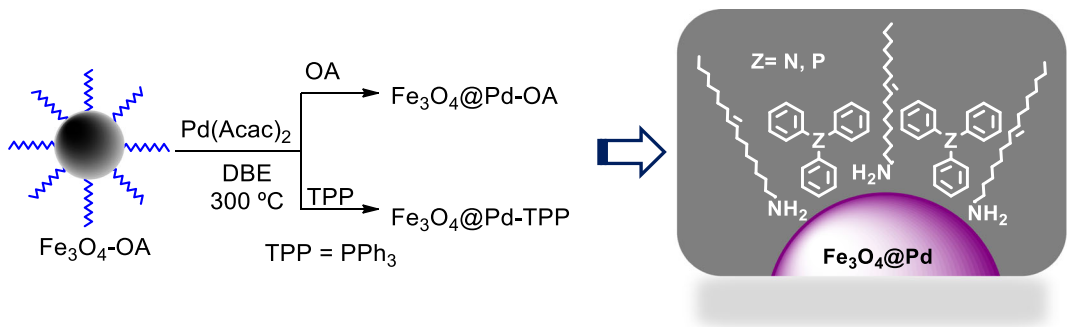

Scheme 1 Schematic representation of the synthetic methodology to obtain core-shell Fe_3O_4@Pd MNPs

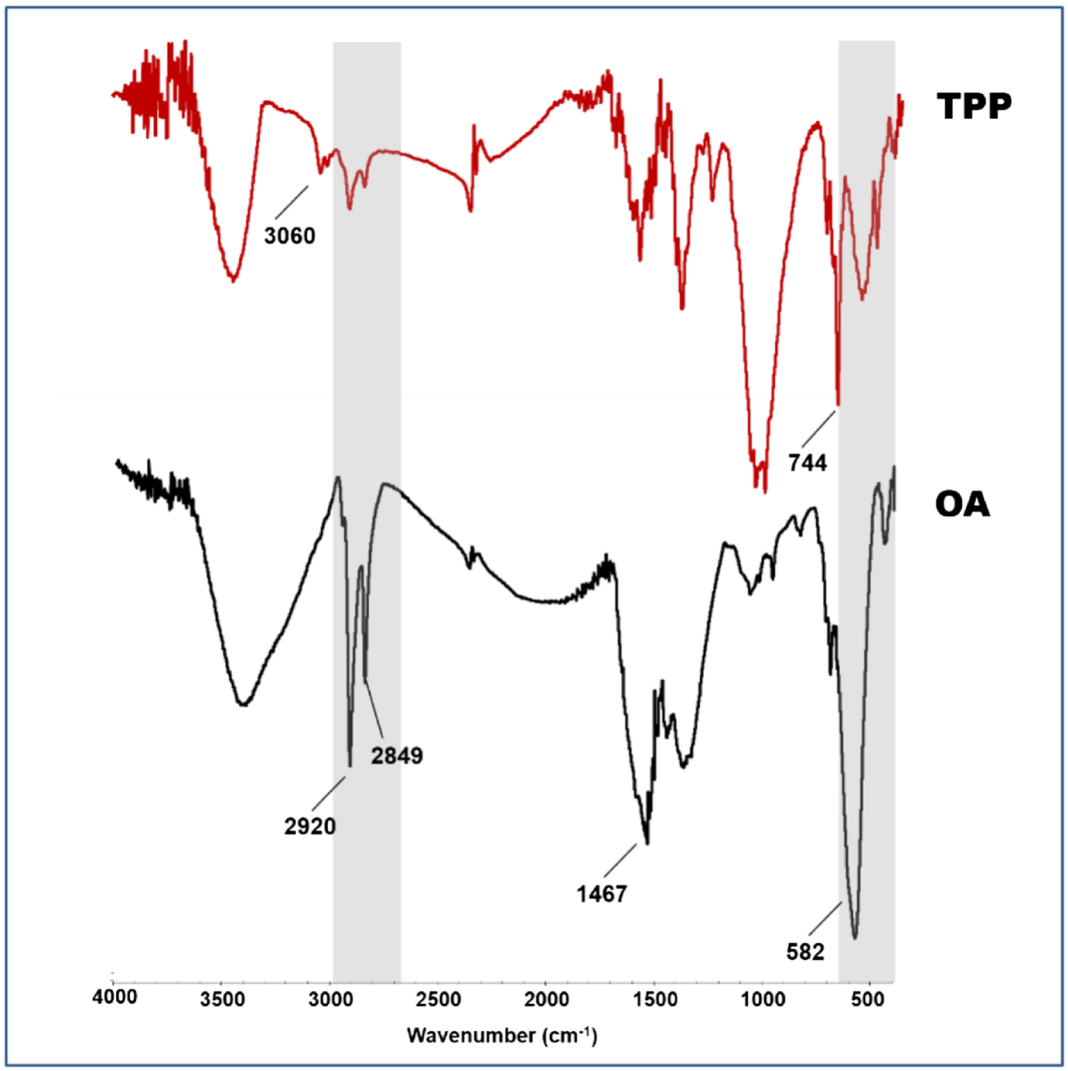

Fig. 1 FT-IR spectra of core-shell Fe_3O_4@Pd MNPs stabilized with OA and TPP

TPP, an additional experiment was performed employing triphenylamine (TPA) as ligand (Fig. SI1). Once again, the MNPs obtained in presence of TPA exhibited the additional phase of PdO.

Therefore, the detailed analysis of the PXRD pattern reveals that the presence of OA in the deposition step of $Pd(Acac)_2$ is required in order to obtain a shell of pure Pd(0) over the surface of the nanoparticle. When employing TPP or TPA in the deposition step, oxidation of Pd shell took place. Furthermore, the presence of OA was observed in all MNPs by FT-IR analysis. This revealed that neither TPP nor TPA can displace effectively the OA from the MNP surface (for FT-IR spectrum of Fe_3O_4@Pd-TPA, see Fig. S2, Supporting Information). Therefore, the OA has a dual role acting as a reducing agent and a stabilizer not only for magnetic core (Mazumder and Sun 2009; Georgiadou et al. 2014; Xu et al. 2009), but also for protection against oxidation of the Pd(0) shell.

With the aim of investigating the stabilizer effect on the morphology and size of the nanocatalysts, MNPs were analyzed by TEM (Fig. 3). TEM micrographs showed that Fe_3O_4@Pd-OA MNPs were spherical particles with low polydispersity with an average size of 7 ± 1 nm (Fig. 3a). In contrast, nanoparticles with amorphous shape and a larger polydispersity with an average size of 9 ± 6 nm (Fig. 3b) were observed for Fe_3O_4@Pd-TPP MNPs (Fig. 3b). This analysis leads to the

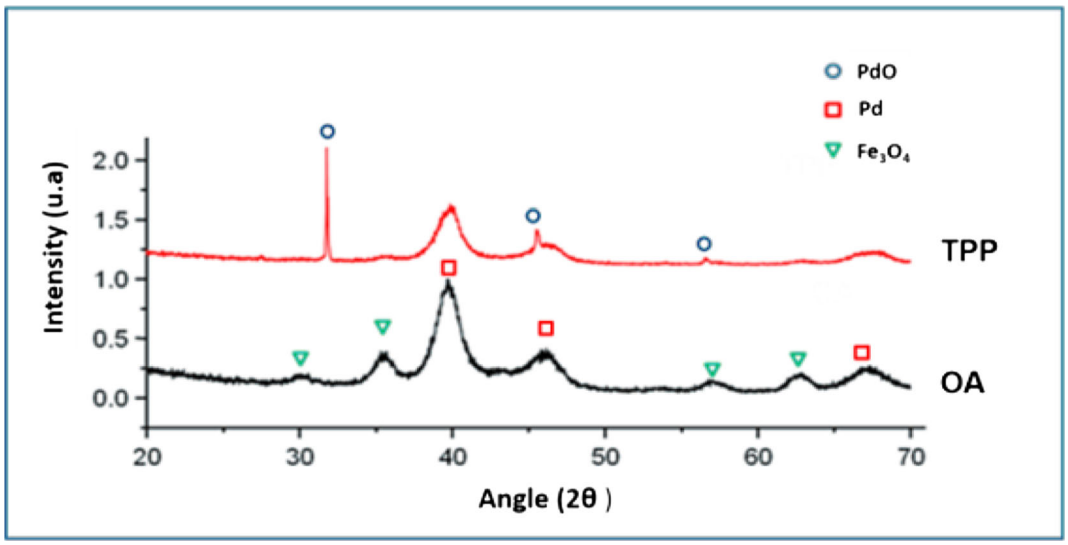

Fig. 2 PXRD pattern of core-shell Fe_3O_4@Pd MNPs stabilized with OA and TPP

conclusion that the presence of TPP during the Pd^{2+} deposition process produced amorphous nanomaterial, in addition to the oxidation of Pd shell.

Catalytic activity of Fe_3O_4@Pd MNPs in C–C coupling reactions

Heck-Mizoroki coupling reaction was selected to evaluate the catalytic activity of MNPs. The reaction between *p*-iodoanisole (**1a**) and styrene (**2a**) was chosen as a model reaction, employing 1.5 mol% of catalyst, 2 equivalents of K_2CO_3 as base and DMF as solvent at 115 °C for 6 h. Under this reaction conditions, Fe_3O_4@Pd-OA catalyst converted substrate **1a** in 97%, while Fe_3O_4@Pd-TPP catalyst gave a lower conversion of 82%. Considering that we demonstrated that MNPs synthesized in presence of OA were spherical in shape with low polydispersity, presented a Pd(0) phase, and also showed more activity as catalysts, Fe_3O_4@Pd-OA were selected for further studies. Different parameters such as reaction time and catalyst loading were optimized, evaluating time dependence conversion at 0.5, 1.5, and 2.8 mol% of Pd (Fig. 4 and Table 1), considering that a Pd content of 20% *w*/*w* for the Fe_3O_4@Pd-OA MNPs (determined by TGA analysis, UV measurements, and confirmed by ICP-MS analysis). This comparative analysis allowed determining the optimal working conditions to perform Heck-Mizoroki coupling reaction with the Fe_3O_4@Pd-OA MNPs.

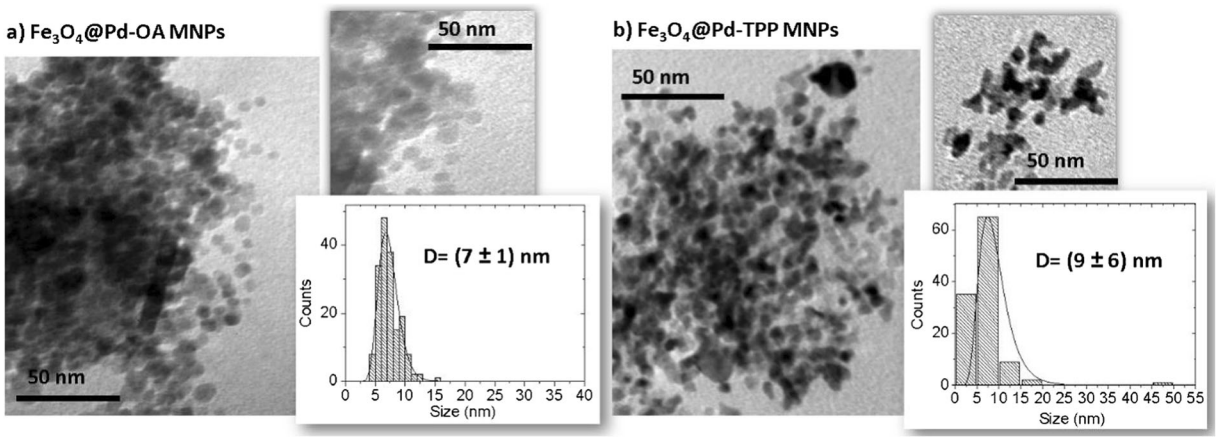

Fig. 3 TEM micrographs for core-shell Fe_3O_4@Pd-OA (**a**) and Fe_3O_4@Pd-TPP (**b**)

Figure 4 shows the time-dependence conversion of **1a** with different amounts of Pd. These studies revealed that substrate **1a** could be converted smoothly into product **3** at a relatively low catalyst loading (0.5 mol%), reaching 100% of conversion after 24 h. When 1.5 mol% of Pd was employed, complete conversion of **1a** was obtained after 6 h. While using almost twice of Pd catalyst (2.8 mol%), only a slight improvement was observed in reaction time from 6 to 4 h. In addition, conversion and selectivity in this reaction were also examined (Table 1).

Analyzing the stereoselectivity of the reaction, it was found that in all cases, *trans* isomer was the major product; however, *gem* and *cis* isomers of alkene **3** were also observed. When 1.5 or 2.8 mol% of catalyst were employed, high conversions in short reaction times with high selectivity (up to 80%) were achieved (entries 1 and 2, Table 1). Furthermore, in order to find the limits of the catalytic system, reactions were performed under a relatively low catalyst loading (0.5 and 0.04 mol% of Pd, entries 3 and 4, Table 1). In these cases, successful conversion and high selectivity were accomplished, with a significantly high TOF number of 79 h^{-1} with 0.04 mol% of Pd (entry 4, Table 1) (Laska et al. 2009). As a negative control, Fe_3O_4-OA MNPs were employed as catalyst. In this case, no conversion was observed (entry 5, Table 1), which suggests that Pd is the active metal for this reaction. Therefore, considering the compromise between catalyst loading and time, the

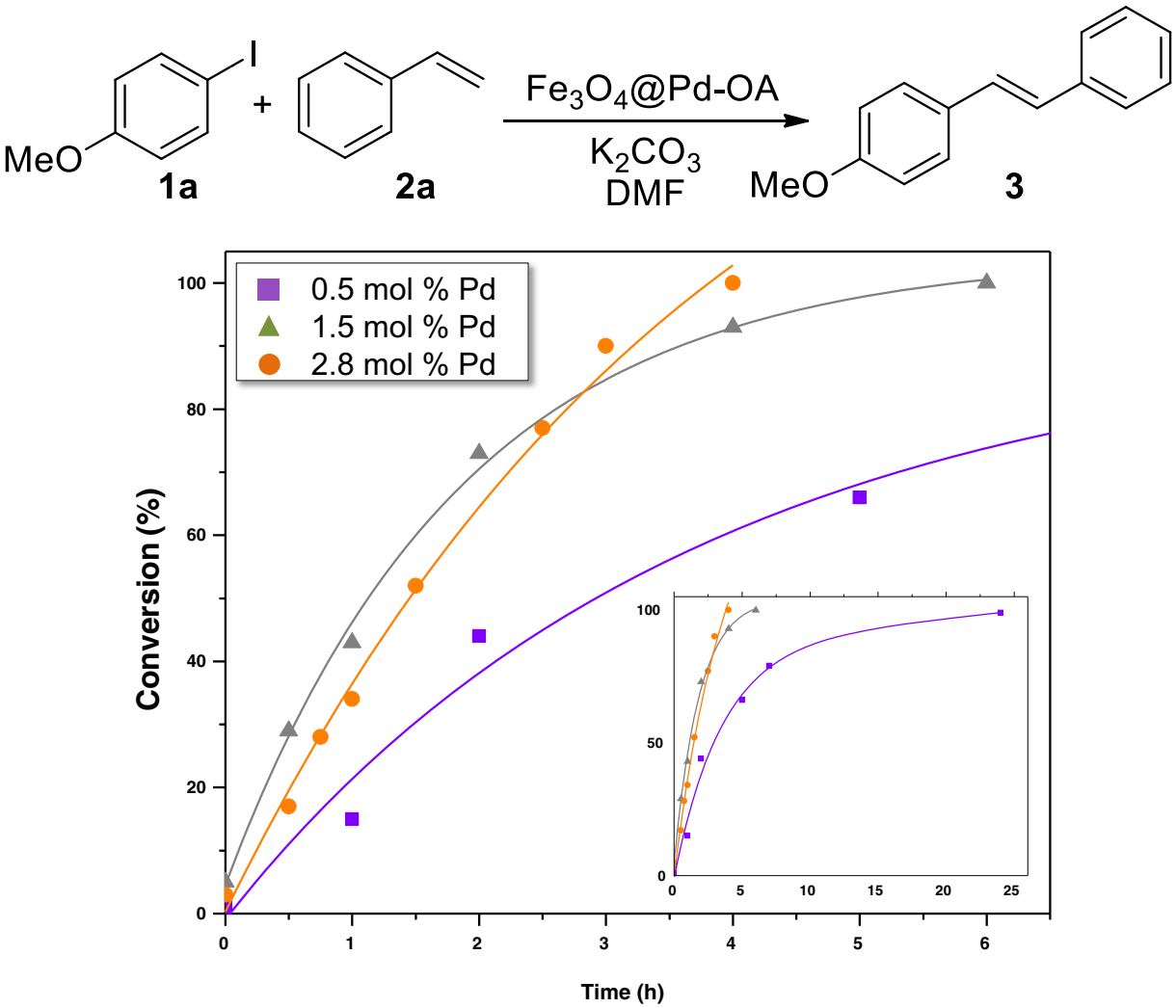

Fig. 4 Time-dependence conversion of **1a** with different Pd loadings

Table 1 Evaluation of reaction conditions for Heck-Mizoroki coupling reaction of *p*-iodoanisole (**1a**) and styrene (**2a**) with MNPs Fe_3O_4@Pd-OA in DMF

Entry	mol % Pd	Time (h)	Conv. 1a (%)[a]	TOF (h^{-1})	Selectivity 3 (%)		
					Trans	*Gem*	*Cis*
1	2.8	4	92	8	84	16	–
2	1.5	6	97	11	83	15	2
3	0.5	24	99	8	86	14	–
4	0.04	24	76	79	82	18	–
5[b]	–	6	–	–	–	–	–

Reaction conditions: coupling reaction was carried out with *p*-iodoanisole **1** (1 equiv.), styrene **2** (1.5 equiv.), Fe_3O_4@Pd-OA, K_2CO_3 (2 equiv.), and 2 mL DMF at 115 °C under nitrogen atmosphere

[a] GC yields (average of two or more experiments)

[b] Reaction performed with Fe_3O_4-OA MNPs as catalyst

reaction condition with 1.5 mol% of Pd and 6 h was chosen for further studies.

Due to the promising results obtained with Fe_3O_4@Pd-OA MNP nanocatalyst in Heck-Mizoroki coupling reaction, the scope of this catalytic system was evaluated with different substrates (Table 2).

Stilbene products were obtained from moderate to excellent yields. With electron-rich aryl iodides such as *p*-iodoanisole (**1a**), *p*-iodoaniline (**1b**), and *p*-iodotoluene (**1c**), the corresponding coupling products **3**, **4**, and **5** were obtained with high conversions in 80, 73, and 75% yield (entries 1–3, Table 2). The steric hindrance effect in these reactions was studied by employing *o*-iodotoluene (**1d**) as coupling partner (entry 4, Table 2). In this case, a slight decrease in yield product was observed in comparison with *p*-iodotoluene (**1c**). With an aryl iodide substituted with an electron-withdrawing group, *p*-iodobenzotrifluoride (**1e**), excellent yield was observed (entry 5, Table 2). In all cases, high conversions were achieved after only 6 h.

When the influence of the reactivity of haloarene was investigated, as expected, bromoarene reactivity was lower than that with aryl iodides. Electron-rich substrate *p*-bromoanisole (**1b**) gave only 10% of conversion after 24 h (entry 6, Table 2). With aryl bromide substituted with an electron-withdrawing group *p*-bromobenzophenone (**1 g**), excellent yield for coupling product **8** was obtained after 24 h (entry 8, Table 2). With *p*-bromobenzonitrile (**1h**) as substrate, a negligible amount of stilbene **9** was observed (entry 9, Table 2), in addition with a complex mixture of other non-identified side products (55% of conversion). A different reactivity was exhibited by *p*-bromoacetophenone (**1i**). After only 3 h, excellent yield of coupling product **10** was obtained (entries 10 and 11, Table 2). In this reaction, the atmosphere effect over the catalytic activity was also examined by performing the reaction under air. A slight decrease in the reaction performance was found, since 75% yield of the coupling product **10** was observed after 3 h. With the heterocyclic alkene 4-vinylpiridine (**2b**), a strong inhibition in reactivity was detected with both electron-rich and electron-poor aryl halides (entries 12 and 13, Table 2). Coupling products **11** and **12** were obtained in 44 and 24% yield, with a conversion of only 63 and 35% of substrate **1c** and **1i**. This kind of heterocyclic compounds usually presents some limitations in transition metal-catalysis since they can act as catalyst poison (Xu et al. 2014).

Following a similar trend like the Heck-Mizoroki reaction, *p*-iodoanisole (**1a**) reacted in short reaction time and with excellent yields in the Suzuki-Miyaura cross-coupling reaction, as previously reported (Cappelletti et al. 2015). Expanding the application of Fe_3O_4@Pd-OA, and as a proof of concept, some aryl halides and aryl boronic acids were evaluated in presence of Fe_3O_4@Pd-OA magnetic nanocatalyst (Scheme 2).

In this reaction, negligible steric hindrance was observed when using *o*-methoxyphenylboronic acid (**13b**) as the coupling partner. The cross-coupling product **15** was obtained in 88% yield (Scheme 2). With *p*-bromoacetophenone (**1i**), good yields of the coupling product **17** were obtained after only 3 h, even when the reaction was performed under air atmosphere. The reaction between *p*-bromoacetophenone (**1i**) and boronic acid **13a** produced biaryl product **17** in 82% yield under

Table 2 Heck-Mizoroki coupling reaction with Fe_3O_4@Pd-OA MNPs as catalyst

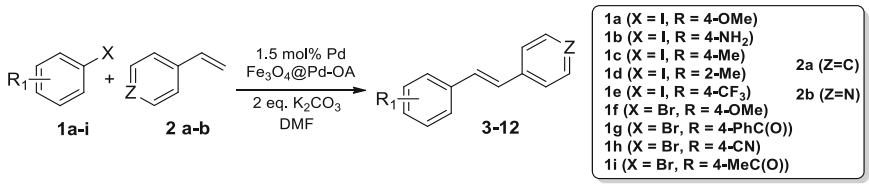

Entry	Substrate	Alkene	Time (h)	Trans Product	Yield Trans (%)	Conv. (%)	TOF (h^{-1})
1	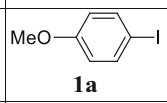 **1a**	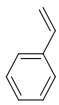 **2a**	6	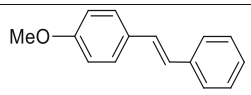	**3:** 80	96	10
2	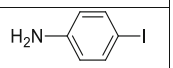 **1b**		6	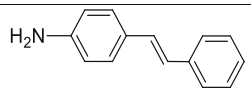	**4:** 73	94	10
3	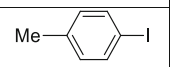 **1c**		6	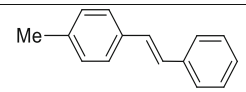	**5:** 75	82	9
4	 **1d**		6	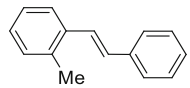	**6:** 68	70	8
5	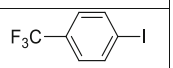 **1e**		6	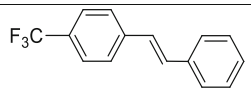	**7:** 89	99	11
6	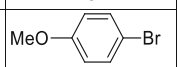 **1f**		24	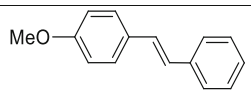	**3:** < 5	10	--
7	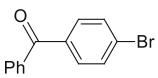 **1g**		6	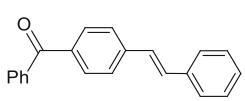	**8:** 28	39	4
8			24		**8:** 93	99	3
9	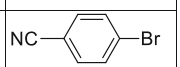 **1h**		24	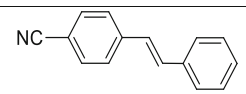	**9:** < 5	55	--
10	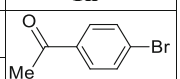 **1i**		3	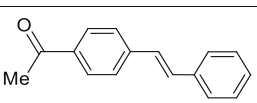	**10:** 86	95	21
11					**10:** 75 [c]	83	18
12	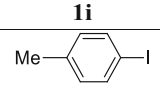 **1c**	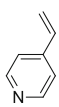 **2b**	6	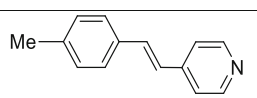	**11:** 44	63	7
13	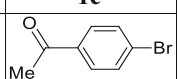 **1i**		24	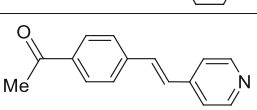	**12:** 24	35	1

[a] Reaction conditions: coupling reaction was carried out with aryl halide (1 equiv.), alkene (1.5 equiv.), Fe_3O_4@Pd-OA (1.5 mol% Pd), base (2 equiv.), and 2 mL DMF at 115 °C under nitrogen atmosphere

[b] GC yields of *trans*-stilbene product (average of two experiments)

[c] Reaction performed under air atmosphere

Scheme 2 Suzuki-Miyaura cross-coupling reaction catalyzed by Fe_3O_4@Pd-OA MNPs

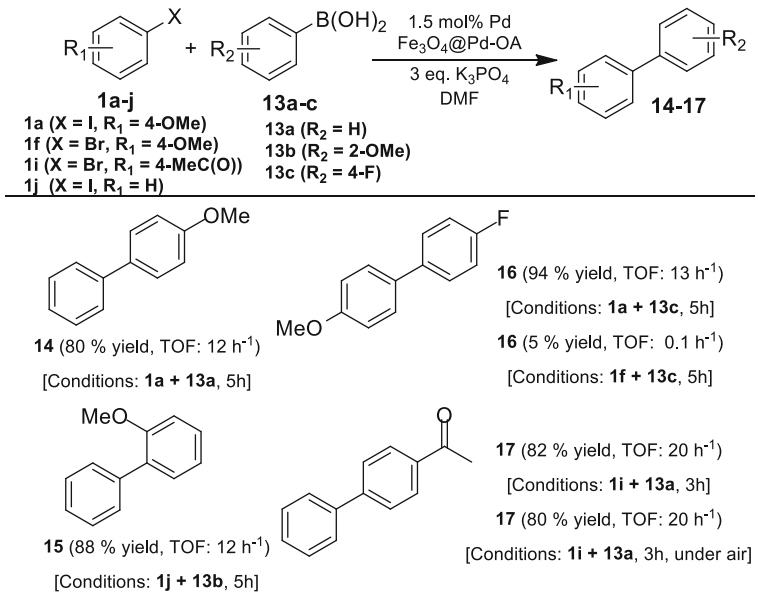

nitrogen and gave 80% yield under air. Unfortunately, electron-rich aryl bromides do not react under these reaction conditions.

Therefore, MNP catalyst presents several advantages such as not suffering deactivation by the action of the air atmosphere, as well as an easy workup, simple product isolation and short reaction time. These notable features demonstrated the benefit of employing this magnetic catalyst. Additionally, Fe_3O_4@Pd-OA MNPs exhibited excellent activity with good TOF values in the coupling reactions studied, higher than those of other magnetic nanocatalysts (Wang et al. 2015; Rafiee et al. 2014; Zhou et al. 2010; Ma et al. 2012).

In order to investigate the recyclability of Fe_3O_4@Pd-OA MNPs catalyst, both Heck-Mizoroki and Suzuki-Miyaura coupling reactions were evaluated employing *p*-iodoanisole (**1a**) as a model substrate. The results are presented in Table 3.

As it is shown, on both reaction systems, Fe_3O_4@Pd-OA catalyst was efficiently recovered by magnetic separation using a neodymium commercial magnet. In Heck-Mizoroki coupling reaction, three cycles could be performed with high conversions, while in the Suzuki-Miyaura cross-coupling process, the catalyst allowed performing four cycles. Regrettably, a decrease in catalyst activity was found after few cycles in both cases.

The loss of the catalytic activity could be associated with Pd leaching from the Fe_3O_4@Pd-OA. To investigate this phenomenon, Pd content was determined in the final reaction mixture for Heck-Mizoroki coupling reaction between **1a** and **2a** by ICP-MS analysis. For this purpose, once the reaction was finished, the organic phase was separated from the catalyst by application of a magnetic external field. The Pd concentration found in the organic phase was 1.9 ± 0.1 ppm, which represents 2.7% of the total Pd content used in the reaction. To evaluate if the leached Pd was an active catalyst in this system, a hot filtration test was performed in Heck-Mizoroki coupling between **1a** and **2a**. As a result of removing the catalyst from the reaction mixture, the reaction was inhibited (Fig. 5), and 2 h later, a slight growth of 5% for product **3** was detected by GC analysis (Supporting information Fig. S3). Therefore, even though magnetic catalyst experiences a leaching process during the reaction, the leached Pd from Fe_3O_4@Pd-OA had negligible catalytic activity.

Besides the small Pd leaching, another possible explanation for the loss of catalytic activity could be addressed to the agglomeration of the MNPs (Kainz et al. 2014). In a first approximation, OA stabilizer could be removed from the catalyst surface by action of organic solvent and temperature. Thus, the initial exposure of MNP surface could produce a positive effect over the catalysis, since more active catalyst surface is available to react. Nevertheless, it could eventually lead to MNP aggregation. To confirm this, TEM measurements of MNPs were performed after the fourth catalytic cycle (Fig. S7, Supporting information). The analysis TEM micrographs revealed that original small and well

Table 3 Recyclability test of Fe_3O_4@Pd-OA MNPs catalyst in Heck-Mizoroki and Suzuki-Miyaura coupling reaction with *p*-iodoanisole (**1a**)

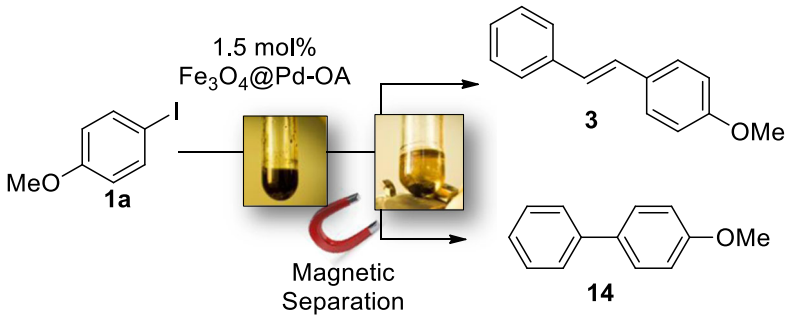

Reaction	Recycling Test (conversion %)			
	Run 1	Run 2	Run 3	Run 4
Heck-Mizoroki [a]	98	96	61	48
Suzuki-Miyaura [b]	87	86	81	63

[a] Reaction conditions for Heck-Mizoroki coupling reaction: the reaction was carried out with arylhalide (1 equiv.), alkene (1.5 equiv.), Fe_3O_4@Pd-OA (1.5 mol% Pd), K_2CO_3 (2 equiv.), and 2 mL DMF at 115 °C under nitrogen atmosphere for 6 h

[b] Reaction conditions for Suzuki-Miyaura coupling reaction: the reaction was carried out with aryl halide (1 equiv.), arylboronic acid (1.5 equiv.), Fe_3O_4@Pd-OA (1.5 mol% Pd), K_3PO_4 (3 equiv.), and 2 mL DMF at 115 °C under nitrogen atmosphere for 5 h

dispersed MNPs, clump into larger aggregates after several reaction cycles (Fig. S7, Supporting information). Therefore, wiping the OA stabilizer from the catalyst surface by action of organic solvent or chemical reaction promotes the aggregation of MNPs, producing coalesces of the catalyst, which leads to a decrease in the catalytic activity.

Catalytic activity of Fe_3O_4@Pd-OA MNPs in hydrogenation of 4-chloronitrobenzene

Additionally, the catalytic activity of Fe_3O_4@Pd-OA MNPs was evaluated in hydrogenation of nitro functional group. Catalytic hydrogenation by transition metal of nitro compounds is one of the most effective methods for industrial production of amines. Therefore, it is important to develop an effective and clean catalysts capable of converting nitro-compounds into NH_2-containing compounds (Kantam et al. 2008; Uberman et al. 2017).

In this sense, hydrogenation of *p*-chloronitrobenzene (**18**) was performed, using sodium borohydride ($NaBH_4$) as an economical hydrogen source (Ganem and Osby 1986). In this reaction, ethanol (EtOH) was

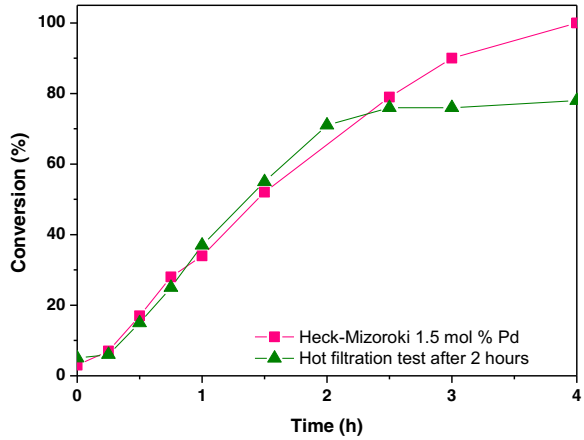

Fig. 5 Hot filtration test in Heck-Mizoroki coupling reaction between *p*-iodoanisole and styrene catalyzed by Fe_3O_4@Pd-OA catalyst

used as solvent at room temperature. Table 4 summarizes the obtained results.

Recently, the use of Fe catalyst in this hydrogenation reaction has been reported (Jagadeesh et al. 2013). However, in the present study, Fe_3O_4-OA MNPs were not active under the reaction conditions studied, since the nitro compound **18** was fully recovered after 30 min of reaction (entry 1, Table 4). On the other hand, the nitro compound **18** was converted to amine **19** in 84% after 30 min, when 4 equivalents of $NaBH_4$ and 0.75 mol% Pd of Fe_3O_4@Pd-OA were employed (entry 2, Table 4). These results proved that Pd is the active metal in hydrogenation reaction by Fe_3O_4@Pd-OA catalyst.

Complete conversion of nitro **18** was observed when Pd loading was raised to 1.5 mol% (entries 3–5, Table 4). Likewise, full conversion of **18** was detected at a shorter reaction time; after 1 min, 92% of conversion of nitrocompound **18** was achieved. Fe_3O_4@Pd-OA provided a TOF value of 3500 h^{-1}. This is an excellent behavior for this type of system. Moreover, this catalyst exhibited high activity in the nitroaromatic reduction under green protocols like EtOH as solvent, room temperature, and low amount of reducing agent. This exceptional catalytic activity in the hydrogenation reaction was even superior as compared with other magnetic catalysts already described in literature (Nasir Baig and Varma 2014; Zhou et al. 2013).

Conclusions

In this study, the effect of different ligands such as OA, TPA, and TPP in the synthesis of Fe_3O_4@Pd MNPs was investigated. It was found that among the stabilizers studied, OA was the only ligand capable of producing spherical MNPs with good size and with a Pd(0) shell around the magnetite core. This could be related to the dual function of OA as a reducing agent and stabilizer in the nanoparticle synthesis. Regarding to TPP and TPA ligands in Fe_3O_4@Pd MNP synthesis, they showed to be unsuitable for the synthesis and stabilization of these magnetic nanocatalysts.

Table 4 Nitroaromatic reduction of *p*-chloronitrobenzene (**18**) catalyzed by Fe_3O_4@Pd-OA

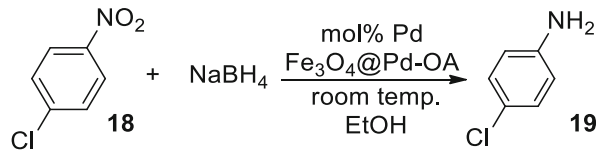

Entry	mol % Pd (catalyst)	Time (min)	% Conversion 18 [b]	TOF (h^{-1})
1	-- (Fe_3O_4-OA)[c]	30	--	--
2	0.75 (Fe_3O_4@Pd-OA)	30	84	223
3	1.5 (Fe_3O_4@Pd-OA)	30	100	132
4		5	100	795
5		1	92	3572

Reaction conditions: the reaction was carried out with *p*-chloronitrobenzene (0.25 mmol), $NaBH_4$ (1 mmol), Fe_3O_4@Pd-OA, and 2 mL EtOH at room temperature

[a] The conversion was determined by GC yield

[b] Reaction performed with Fe_3O_4 as catalyst

Concerning the catalytic activity of the Fe_3O_4@Pd–OA MNPs, they exhibited remarkable properties as nanocatalyst, since high conversions at moderate catalyst loading and in a short reaction time were achieved. It was found that Heck-Mizoroki coupling reaction was effectively catalyzed by core-shell Fe_3O_4@Pd–OA nanocatalyst, obtaining diverse stilbenes derivatives in good yield, high selectivity, and TOF values. C–C bond formation by Suzuki-Miyaura cross-coupling reaction was also investigated presenting promising results. Furthermore, hydrogenation of *p*-chloronitrobenzene took place with great TOF values and under green reaction protocols using these core-shell nanoparticles.

In addition, recyclability of Fe_3O_4@Pd-OA MNPs was evaluated in C–C coupling reaction. Fe_3O_4@Pd-OA nanocatalysts were separated from the reaction mixture with a commercial magnet in a simple procedure with small Pd leaching, showing good activity for at least four cycles. Nevertheless, the sole presence of OA ligand is not effective enough to extent the MNP efficacy to carry out several cycles, probably due to a coalesce process as a consequence of the ligand dissociation during the catalytic cycles. Further research concerning to stabilizer effect over MNP stabilization and catalytic activity are currently under study.

Acknowledgements The authors acknowledge research support from CONICET, FONCYT, and SECYT. C. B. gratefully thanks National University Council for the CIN-fellowship, and CONICET for her fellowship. A. L. C. thanks CONICET for his fellowship.

Funding This study was funded by Secyt-UNC, CONICET, and Foncyt-Mincyt.

Compliance with ethical standards

Conflict of interest The authors declare that they have no conflict of interest.

References

Alacid E, Nájera C (2009) General reaction conditions for the palladium-catalyzed vinylation of aryl chlorides with potassium alkenyltrifluoroborates. J Org Chem 74:8191–8195. https://doi.org/10.1021/jo901681s

Astruc D (2007) Palladium nanoparticles as efficient green homogeneous and heterogeneous carbon-carbon coupling precatalysts: a unifying view. Inorg Chem 46:1884–1894. https://doi.org/10.1021/ic062183h

Astruc D, Lu F, Aranzaes JR (2005) Nanoparticles as recyclable catalysts: the frontier between homogeneous and heterogeneous catalysis. Angew Chem Int Ed 44:7852–7872. https://doi.org/10.1002/anie.200500766

Atashkar B, Rostami A, Tahmasbi B (2013) Magnetic nanoparticle-supported guanidine as a highly recyclable and efficient nanocatalyst for the cyanosilylation of carbonyl compounds. Catal Sci Technol 3:2140–2146 http://pubs.rsc.org/en/content/articlehtml/2013/cy/c3cy00190c

Beletskaya IP, Cheprakov AV (2009) Focus on catalyst development and ligand design. In: Oestreich M (ed) The Mizoroki-heck reaction. John Wiley & Sons, Ltd, Chichester, pp 51–132. https://doi.org/10.1002/9780470716076.ch2

Bi Y, Lu G (2003) Catalytic CO oxidation over palladium supported NaZSM-5 catalysts. Appl Catal B Environ 41:279–286. https://doi.org/10.1016/S0926-3373(02)00166-2

Cantillo D, Moghaddam MM, Kappe CO (2013) Hydrazine-mediated reduction of nitro and azide functionalities catalyzed by highly active and reusable magnetic iron oxide nanocrystals. J Org Chem 78:4530–4542. https://doi.org/10.1021/jo400556g

Cappelletti AL, Uberman PM, Martin SE, Saleta ME, Troiani HE, Sánchez RD, Carbonio RE, Strumia MC (2015) Synthesis, characterization, and nanocatalysis application of core-shell superparamagnetic nanoparticles of Fe_3O_4@Pd. Aust J Chem 68:1492–1501. https://doi.org/10.1071/CH14722

Ceylan S, Friese C, Lammel C, Mazac K, Kirschning A (2008) Inductive heating for organic synthesis by using functionalized magnetic nanoparticles inside microreactors. Angew Chem Int Ed 47:8950–8953. https://doi.org/10.1002/anie.200801474

Deraedt C, Astruc D (2014) "Homeopathic" palladium nanoparticle catalysis of cross carbon-carbon coupling reactions. Acc Chem Res 47:494–503. https://doi.org/10.1021/ar400168s

Dounay AB, Overman LE (2003) The asymmetric intramolecular heck reaction in natural product total synthesis. Chem Rev 103:2945–2963. https://doi.org/10.1021/cr020039h

Ferrando R, Jellinek J, Johnston RL (2008) Nanoalloys: from theory to applications of alloy clusters and nanoparticles. Chem Rev 108:845–910. https://doi.org/10.1021/cr040090g

Fihri A, Bouhrara M, Nekoueishahraki B, Basset JM, Polshettiwar V (2011) Nanocatalysts for Suzuki cross-coupling reactions. Chem Soc Rev 40:5181–5203

Frey NA, Peng S, Cheng K, Sun S (2009) Magnetic nanoparticles: synthesis, functionalization, and applications in bioimaging and magnetic energy storage. Chem Soc Rev 38:2532–2542. https://doi.org/10.1039/b815548h

Fu GC (2008) The development of versatile methods for palladium-catalyzed coupling reactions of aryl electrophiles through the use of $P(t\text{-}Bu)_3$ and PCy_3 as ligands. Acc Chem Res 41:1555–1564. https://doi.org/10.1021/ar800148f

Ganem B, Osby JO (1986) Synthetically useful reactions with metal boride and aluminide catalysts. Chem Rev 86:763–780. https://doi.org/10.1021/cr00075a003

García CS, Uberman PM, Martín SE (2017) An effective Pd nanocatalyst in aqueous media: stilbene synthesis by Mizoroki-heck coupling reaction under microwave irradiation. Beilstein J Org Chem 13:1717–1727 https://www.beilstein-journals.org/bjoc/articles/13/166

Garrett CE, Prasad K (2004) The art of meeting palladium specifications in active pharmaceutical ingredients produced by Pd-catalyzed reactions. Adv Synth Catal 346:889–900. https://doi.org/10.1002/adsc.200404071

Georgiadou V, Kokotidou C, le Droumaguet B, Carbonnier B, Choli-Papadopoulou T, Dendrinou-Samara C (2014) Oleylamine as a beneficial agent for the synthesis of $CoFe_2O_4$ nanoparticles with potential biomedical uses. Dalton Trans 43:6377–6388

Hong RY, Pan TT, Li HZ (2006) Microwave synthesis of magnetic Fe_3O_4 nanoparticles used as a precursor of nanocomposites and ferrofluids. J Magn Magn Mater 303:60–68. https://doi.org/10.1016/j.jmmm.2005.10.230

Jacinto MJ, Kiyohara PK, Masunaga SH, Jardim RF, Rossi LM (2008) Recoverable rhodium nanoparticles: synthesis, characterization and catalytic performance in hydrogenation reactions. Appl Catal A Gen 338:52–57. https://doi.org/10.1016/j.apcata.2007.12.018

Jagadeesh RV, Surkus AE, Junge H, Pohl MM, Radnik J, Rabeah J, Huan H, Schunemann V, Bruckner A, Beller M (2013) Nanoscale Fe_2O_3-based catalysts for selective hydrogenation of Nitroarenes to anilines. Science 342:1073–1076

Jin MJ, Lee DH (2010) A practical heterogeneous catalyst for the Suzuki, Sonogashira, and Stille coupling reactions of unreactive aryl chlorides. Angew Chem Int Ed 49:1119–1122. https://doi.org/10.1002/anie.200905626/full

Kainz QM, Reiser O (2014) Polymer- and dendrimer-coated magnetic nanoparticles as versatile supports for catalysts, scavengers, and reagents. Acc Chem Res 47:667–677. https://doi.org/10.1021/ar400236y

Kainz QM, Linhardt R, Grass RN, Vilé G, Pérez-Ramírez J, Stark WJ, Reiser O (2014) Palladium nanoparticles supported on magnetic carbon-coated cobalt nanobeads: highly active and recyclable catalysts for alkene hydrogenation. Adv Funct Mater 24:2020–2027. https://doi.org/10.1002/adfm.201303277

Kantam ML, Chakravarti R, Pal U, Sreedhar B, Bhargava S (2008) Nanocrystalline magnesium oxide-stabilized palladium(0): an efficient and reusable catalyst for selective reduction of nitro compounds. Adv Synth Catal 350:822–827. https://doi.org/10.1002/adsc.200800018

Kantchev EAB, O'Brien CJ, Organ MG (2007) Palladium complexes of N-heterocyclic carbenes as catalysts for cross-coupling reactions - a synthetic chemist's perspective. Angew Chem Int Ed 46:2768–2813. https://doi.org/10.1002/anie.200601663

Kim M, Song H (2014) Precise adjustment of structural anisotropy and crystallinity on metal–Fe_3O_4 hybrid nanoparticles and its influence on magnetic and catalytic properties. J Mater Chem C 2:4997–5004 http://xlink.rsc.org/?DOI=c4tc00416g

Laska U, Frost CG, Price GJ, Plucinski PK (2009) Easy-separable magnetic nanoparticle-supported Pd catalysts: kinetics, stability and catalyst re-use. J Catal 268:318–328. https://doi.org/10.1016/j.jcat.2009.10.001

Leadbeater NE, Marco M (2002) Ligand-free palladium catalysis of the Suzuki reaction in water using microwave heating. Org Lett 4:2973–2976. https://doi.org/10.1021/ol0263907

Lee J, Zhang S, Sun S (2013) High-temperature solution-phase syntheses of metal-oxide nanocrystals. Chem Mater 25:1293–1304. https://doi.org/10.1021/cm3040517

Li P, Wang L, Zhang L, Wang GW (2012) Magnetic nanoparticles-supported palladium: a highly efficient and reusable catalyst for the Suzuki, Sonogashira, and heck reactions. Adv Synth Catal 354:1307–1318. https://doi.org/10.1002/adsc.201100725

Liu J, Peng X, Sun W, Zhao Y, Xia C (2008) Magnetically separable Pd catalyst for carbonylative sonogashira coupling reactions for the synthesis of α,β-alkynyl ketones. Org Lett 10:3933–3936. https://doi.org/10.1021/ol801478y

Lyon JL, Fleming DA, Stone MB, Schiffer P, Williams ME (2004) Synthesis of Fe oxide Core/au shell nanoparticles by iterative hydroxylamine seeding. Nano Lett 4:719–723. https://doi.org/10.1021/nl035253f

Ma M, Zhang Q, Yin D, Dou J, Zhang H, Xu H (2012) Preparation of high-magnetization Fe_3O_4–NH_2–Pd (0) catalyst for heck reaction. Catal Commun, 17:168–172. http://www.sciencedirect.com/science/article/pii/S1566736711004055\nhttp://linkinghub.elsevier.com/retrieve/pii/S1566736711004055

Martin R, Buchwald SL (2008) Palladium-catalyzed Suzuki-Miyaura cross-coupling reactions employing dialkylbiaryl phosphine ligands. Acc Chem Res 41:1461–1473. https://doi.org/10.1021/ar800036s

Mazumder V, Sun S (2009) Oleylamine-mediated synthesis of Pd nanoparticles for catalytic formic acid oxidation. J Am Chem Soc 131:4588–4589. https://doi.org/10.1021/ja9004915

De Meijere A, Diederich F (2004) In: de Meijere A, Diederich F (eds) Metal-Catalyzed Cross-Coupling Reactions. Wiley-VCH Verlag GmbH, Weinheim. https://doi.org/10.1002/9783527619535

Metin Ö, Ho SF, Alp C, Can H, Mankin MN, Gültekin MS, Chi M, Sun S (2013) Ni/Pd core/shell nanoparticles supported on graphene as a highly active and reusable catalyst for Suzuki-Miyaura cross-coupling reaction. Nano Res 6:10–18. https://doi.org/10.1007/s12274-012-0276-4

Mori K, Yamashita H (2011) Design of colloidal and supported metal nanoparticles: their synthesis, characterization, and catalytic application. J Jpn Pet Inst 54:1–14 https://www.jstage.jst.go.jp/article/jpi/54/1/54_1_1/_article

Nasir Baig RB, Varma RS (2014) Magnetic carbon-supported palladium nanoparticles: an efficient and sustainable catalyst for hydrogenation reactions. ACS Sustain Chem Eng 2:2155–2158. https://doi.org/10.1021/sc500341h

Nasir Baig RB, Nadagouda MN, Varma RS (2015) Magnetically retrievable catalysts for asymmetric synthesis. Coord Chem Rev 287:137–156 http://xlink.rsc.org/?DOI=C2CC35663E

Polshettiwar V (2013) Nanomaterials in catalysis . Edited by Philippe Serp and Karine Philippot. https://doi.org/10.1002/anie.201305828

Polshettiwar V, Varma RS (2010) Green chemistry by nano-catalysis. Green Chem 12:743–754. https://doi.org/10.1039/B921171C

Polshettiwar V, Baruwati B, Varma RS (2009) Nanoparticle-supported and magnetically recoverable nickel catalyst: a robust and economic hydrogenation and transfer hydrogenation protocol. Green Chem 11:127–131 http://xlink.rsc.org/?DOI=B815058C

Polshettiwar V, Luque R, Fihri A, Zhu H, Bouhrara M, Basset JM (2011) Magnetically recoverable nanocatalysts. Chem Rev 111:3036–3075. https://doi.org/10.1021/cr100230z

Quinteros GJ, Uberman PM, Martín SE (2015) Bulky monodentate biphenylarsine ligands: synthesis and evaluation of their structure effects in the palladium-catalyzed heck reaction. Eur J Org Chem 2015:2698–2705. https://doi.org/10.1002/ejoc.201403658

Rafiee E, Ataei A, Nadri S, Joshaghani M, Eavani S (2014) Combination of palladium and oleic acid coated-magnetite particles: characterization and using in heck coupling reaction with magnetic recyclability. Inorg Chim Acta 409:302–309 http://linkinghub.elsevier.com/retrieve/pii/S0020169313005276

Rosario-Amorinâ D et al (2009) Dendron-functionalized core-shell superparamagnetic nanoparticles: magnetically recoverable and reusable catalysts for Suzuki cross-coupling reactions. Chem Eur J 15:12636–12643. https://doi.org/10.1002/chem.200901866

Rossi LM, Costa NJS, Silva FP, Wojcieszak R (2014) Magnetic nanomaterials in catalysis: advanced catalysts for magnetic separation and beyond. Green Chem 16:2906–2933 http://xlink.rsc.org/?DOI=c4gc00164h

Sahoo AK et al (2004) Cross-coupling of triallyl(aryl)silanes with aryl bromides and chlorides: an alternative convenient biaryl synthesis. Adv Synth Catal 346:1715–1727. https://doi.org/10.1002/adsc.200404188

Senapati KK, Roy S, Borgohain C, Phukan P (2012) Palladium nanoparticle supported on cobalt ferrite: an efficient magnetically separable catalyst for ligand free Suzuki coupling. J Mol Catal A Chem 352:128–134. https://doi.org/10.1016/j.molcata.2011.10.022

Shylesh S, Wang L, Thiel WR (2010) Palladium(II)-phosphine complexes supported on magnetic nanoparticles: filtration-free, recyclable catalysts for Suzuki-Miyaura cross-coupling reactions. Adv Synth Catal 352:425–432. https://doi.org/10.1002/adsc.200900698

Sobhani S, Pakdin-Parizi Z (2014) Palladium-DABCO complex supported on γ-Fe_2O_3 magnetic nanoparticles: a new catalyst for CC bond formation via Mizoroki-heck cross-coupling reaction. Appl Catal A Gen 479:112–120 http://www.sciencedirect.com/science/article/pii/S0926860X14002695

Sun B, Hoshino J, Jermihov K, Marler L, Pezzuto JM, Mesecar AD, Cushman M (2010) Design, synthesis, and biological evaluation of resveratrol analogues as aromatase and quinone reductase 2 inhibitors for chemoprevention of cancer. Bioorg Med Chem 18:5352–5366 http://linkinghub.elsevier.com/retrieve/pii/S096808961000461X

Torborg C, Beller M (2009) Recent applications of palladium-catalyzed coupling reactions in the pharmaceutical, agrochemical, and fine chemical industries. Adv Synth Catal 351:3027–3043. https://doi.org/10.1002/adsc.200900587

Uberman PM, García CS, Rodríguez JR, Martín SE (2017) PVP-Pd nanoparticles as efficient catalyst for nitroarene reduction under mild conditions in aqueous media. Green Chem 19:739–748 http://xlink.rsc.org/?DOI=C6GC02710E

Wang D, Yang P, Zhu Y (2014a) Growth of Fe_3O_4 nanoparticles with tunable sizes and morphologies using organic amine. Mater Res Bull 49:514–520 http://www.sciencedirect.com/science/article/pii/S0025540813007630

Wang P, Liu H, Liu M, Li R, Ma J (2014b) Immobilized Pd complexes over HMMS as catalysts for heck cross-coupling and selective hydrogenation reactions. New J Chem 38:1138–1143 http://xlink.rsc.org/?DOI=c3nj01108a

Wang D, Liu W, Bian F, Yu W (2015) Magnetic polymer nanocomposite-supported Pd: an efficient and reusable catalyst for the heck and Suzuki reactions in water. New J Chem 39:2052–2059 http://xlink.rsc.org/?DOI=C4NJ01581A

Xu Z, Hou Y, Sun S (2007) Magnetic core/shell Fe_3O_4/au and Fe_3O_4/au/ag nanoparticles with tunable plasmonic properties. J Am Chem Soc 129:8698–8699. https://doi.org/10.1021/ja073057v

Xu Z, Shen C, Hou Y, Gao H, Sun S (2009) Oleylamine as both reducing agent and stabilizer in a facile synthesis of magnetite nanoparticles. Chem Mater 21:1778–1780. https://doi.org/10.1021/cm802978z

Xu T, Zhang Q, Jiang D, Liang Q, Lu C, Cen J, Li X (2014) Thermal oxidation to regenerate sulfone poisoned Pd-based catalyst: effect of the valence of sulfur. RSC Adv 4:33347–33354 http://xlink.rsc.org/?DOI=C4RA03546A

Yin L, Liebscher J (2007) Carbon-carbon coupling reactions catalyzed by heterogeneous palladium catalysts. Chem Rev 107:133–173. https://doi.org/10.1021/cr0505674

Zaleska-Medynska A, Marchelek M, Diak M, Grabowska E (2016) Noble metal-based bimetallic nanoparticles: the effect of the structure on the optical, catalytic and photocatalytic properties. Adv Colloid Interf Sci 229:80–107. https://doi.org/10.1016/j.cis.2015.12.008

Zhang F, Jin J, Zhong X, Li S, Niu J, Li R, Ma J (2011) Pd immobilized on amine-functionalized magnetite nanoparticles: a novel and highly active catalyst for hydrogenation and heck reactions. Green Chem 13:1238–1243. https://doi.org/10.1039/C0GC00854K

Zhang D et al (2012a) Magnetically recyclable nanocatalysts (MRNCs): a versatile integration of high catalytic activity and facile recovery. Nano 4:6244–6255 http://xlink.rsc.org/?DOI=c2nr31929b

Zhang F, Niu J, Wang H, Yang H, Jin J, Liu N, Zhang Y, Li R, Ma J (2012b) Palladium was supported on superparamagnetic nanoparticles: a magnetically recoverable catalyst for heck reaction. Mater Res Bull 47:504–507. https://doi.org/10.1016/j.materresbull.2011.10.030

Zhou L, Gao C, Xu W (2010) Robust Fe_3O_4/SiO_2-Pt/au/Pd magnetic nanocatalysts with multifunctional hyperbranched polyglycerol amplifiers. Langmuir 26:11217–11225. https://doi.org/10.1021/la100556p

Zhou J, Dong Z, Yang H, Shi Z, Zhou X, Li R (2013) Pd immobilized on magnetic chitosan as a heterogeneous catalyst for acetalization and hydrogenation reactions. Appl Surf Sci 279:360–366. https://doi.org/10.1016/j.apsusc.2013.04.113

Zhu Y, Stubbs LP, Ho F, Liu R, Ship CP, Maguire JA, Hosmane NS (2010) Magnetic nanocomposites: a new perspective in catalysis. ChemCatChem 2:365–374. https://doi.org/10.1002/cctc.200900314